

# Three-phase Resonant Inverter for Wireless Power Transfer

Mariusz Bojarski, Erdem Asa, and Dariusz Czarkowski  
 NYU Polytechnic School of Engineering  
 Brooklyn, New York, USA  
 mb4496@nyu.edu, ea1145@nyu.edu, dc1677@nyu.edu

**Abstract**—A three-phase resonant inverter for wireless power transfer applications is presented in this paper. A phase-frequency hybrid control strategy is proposed as an alternative to the traditional frequency and phase control methods. An experimental prototype of the three-phase resonant inverter was built and connected with wireless power link and rectifier. The hybrid phase-frequency control strategy was implemented and compared with frequency control at the output power up to 10 kW. The experimental results show that the proposed inverter can operate within the desired frequency range with high efficiency while regulating output from zero to maximum.

## I. INTRODUCTION

Efficient wireless transfer systems have been recently receiving a growing attention for their numerous potential applications [1]-[3]. With a proper coil winding and magnetic circuit design, the overall efficiency of the system can be increased by minimizing conduction and switching losses [4]-[6]. The recently published studies in wireless energy transfer deal with optimization and design concerns of the system resonant and magnetic coil parameters [7]-[8]. However, there has been little investigation on high power applications and their effect on the wireless system performance [9]-[12]. KAIST has shown a great progress achieving up to 100 kW output power for the dynamic charging of buses [13]-[14]. The achieved system efficiency was, however, up to 80%. In addition, for the commercial applications, electric vehicle charging products are available in the marketplace. Wireless Advance Vehicle Electrification (WAVE) Company establishes an inductive power transfer up to 50 kW at around 90% efficiency with 20 cm clearance [15].

This paper presents a three-phase inverter with hybrid control approach for high power wireless energy transfer applications. A laboratory prototype has been developed and the system has been tested with up to 10 kW of output power. The system comparison has been also supplied with the traditional control approaches. The recommended system with the controller achieves high efficiency, above the 90%, in all load conditions.

## II. CIRCUIT DESCRIPTION

A dc-dc wireless power transfer system with a three-phase inverter is shown in Fig. 1. It consists of a dc input voltage source  $V_I$ , three switching legs (phases), three intercell transformers  $ICT$ , a wireless power link, impedance matching auto-transformer, full bridge current driven rectifier, and an

dc load resistance  $R_L$ . Each intercell transformer has two windings, which are connected as shown in the figure. The wireless power link consist of two identical coils  $L$  and two series resonant capacitors  $C$ . These coils are coupled with each other with the coupling factor  $K$ .

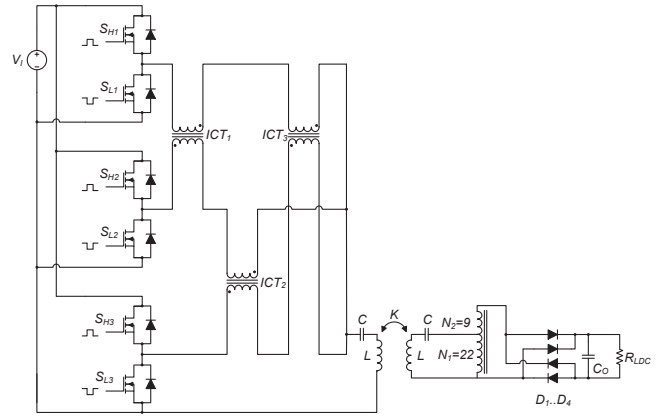


Fig. 1. Three-phase inverter with a wireless power link, impedance matching transformer, rectifier and resistive load.

The efficiency of the wireless power link depends on its load resistance [16]. Thus, the impedance matching auto-transformer is used on the secondary side. It allows to optimize for the particular load and coupling factor without redesigning the wireless power link. The implemented here three-phase inverter is a variant of a multiphase series resonant inverter introduced in [17].

## III. HYBRID CONTROL METHODS

There are two traditional control methods for resonant converters, which provide output regulation, namely, the frequency and the phase control. They have, however, well-known disadvantages. The frequency control requires high tuning resolution close to the resonant frequency. On the other hand, at low power, it requires operation at a frequency much higher than the resonant frequency, which usually results in a poor efficiency at light loads. Moreover, the frequency control is highly non-linear, which leads to a significant difference of gain for light and heavy loads. These problems can be solved by the phase control, which allows for operation at a constant frequency. Nevertheless, the phase control requires operating at a frequency high enough to obtain the ZVS for the whole regulation range and various loads. It reduces the efficiency and limits the output power.

A solution to the problems described above is a hybrid control strategy. Combination of the two traditional control methods results in a phase-frequency control. The principle of operation is to utilize the phase shift for regulating output and the frequency to operate as close to the resonant frequency as possible. There is an important constrain on the operating frequency. It must assure that the load for all switching legs is inductive with a certain minimum phase angle between voltage and current. This is the necessary condition to obtain a zero-voltage turn-on. This concept was introduced in [18]. In this paper, it is expanded to the three-phase inverter in which two control phase shifts are controlled independently.

#### IV. EXPERIMENTAL VERIFICATION

A 10 kW experimental prototype of the proposed inverter was built and tested. A summary of parameters and component values of the prototype is presented in Table I. The  $L_m$  and  $L_l$  are magnetizing and leakage inductance of the intercell transformer respectively. The  $K$  is coupling factor between primary and secondary coil and  $D$  is a distance between those coils. Both coils are identical and tuned with series resonant capacitors to the resonant frequency  $f_o$ . They are coreless and has dimension of 60 by 90 cm.  $N_1$  and  $N_2$  are number of turns of the impedance matching auto-transformer as marked in Fig. 1. In the result, the wireless power link sees two times lower impedance.

TABLE I  
PARAMETERS FOR EXPERIMENTAL PROTOTYPE

Parameter	Value	Unit	Parameter	Value	Unit
$f_o$	82	kHz	$C$	125	nF
$V_I$	400	V	$L_m$	20	$\mu$ H
$L$	30	$\mu$ H	$L_l$	1.5	$\mu$ H
$K$	0.2	-	$D$	20	cm
$N_1$	22	-	$N_2$	9	-

Six IPW65R041CFD MOSFETs were used for the inverter prototype. 1 nF capacitors were added at the output of each switching leg of the inverter to alleviate high  $dv/dt$  at turn-off. The inverter with wireless power link was loaded with a Class D full-bridge current-driven rectifier with resistive load. The rectifier was built using four DSEI2X101-06A diodes. The intercell transformers (ICTs) were built using 0077101A7 cores from Magnetics. The resonant capacitor was constructed by paralleling 125 pieces of 1 nF capacitors rated for 2 kV. The inverter was tested with resistive load. A three values of load resistance were used: 12  $\Omega$ , 16  $\Omega$ , and 20  $\Omega$ .

Two control strategies are implemented for the experimental comparison. The first one is the frequency control. The second one is the phase-frequency hybrid control. The obtained experimental results are presented in Figs. 2-7. Phase voltage and resonant circuit current waveforms are shown in Figs. 2-4 for the hybrid control and 12  $\Omega$  load resistance. Fig. 2 shows waveforms recorded at the high output power of 9 kW. Fig. 3 shows waveforms for a medium output power of 5 kW. It can be seen that two phases are in phase and regulation is performed by the third one. Fig. 4 illustrate operation at 1 kW of output power. At this power level, phase shift between two phases is fixed to 120 $^\circ$  and regulation is done by the third one.

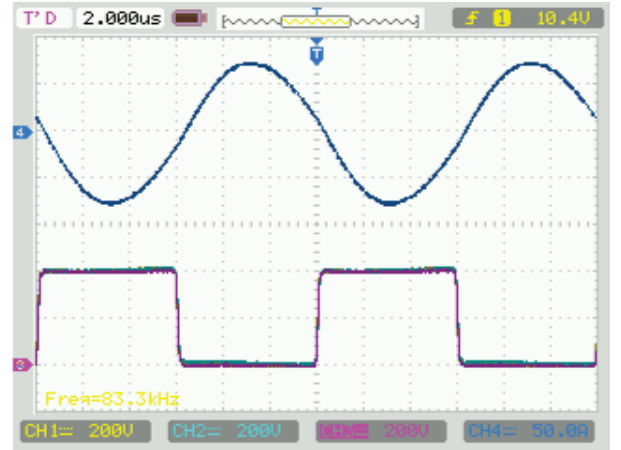


Fig. 2. Measured waveforms of phase voltages and output current for output power below 9 kW. Channels 1 to 3 are phase voltages (200 V/div.), channel 4 is the primary coil current (50 A/div.).

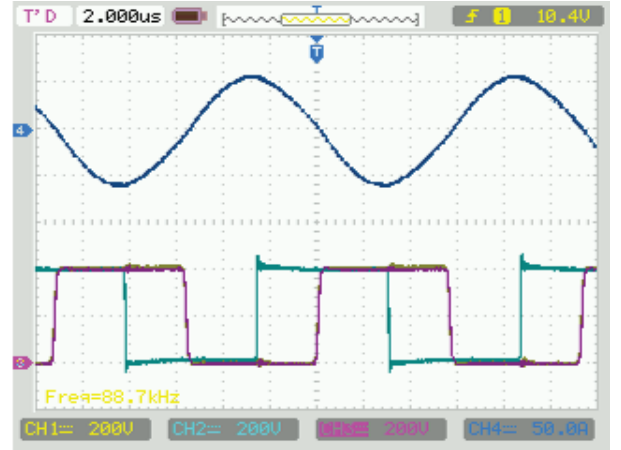


Fig. 3. Measured waveforms of phase voltages and output current for output power of 5 kW. Channels 1 to 3 are phase voltages (200 V/div.), channel 4 is the primary coil current (50 A/div.).

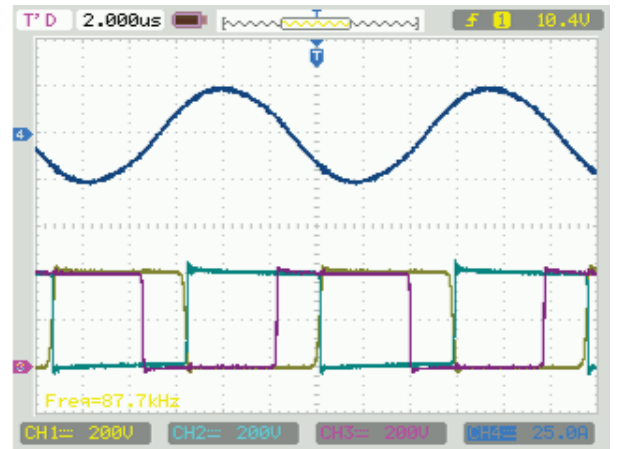


Fig. 4. Measured waveforms of phase voltages and output current for output power of 1 kW. Channels 1 to 3 are phase voltages (200 V/div.), channel 4 is the primary coil current (25 A/div.).

It is important that the operating frequency does not change much while the output power is regulated. It can be also seen that voltage waveform slopes are smooth and there are almost no oscillations after switching which means that all phases are working at ZVS conditions regardless of the output power level.

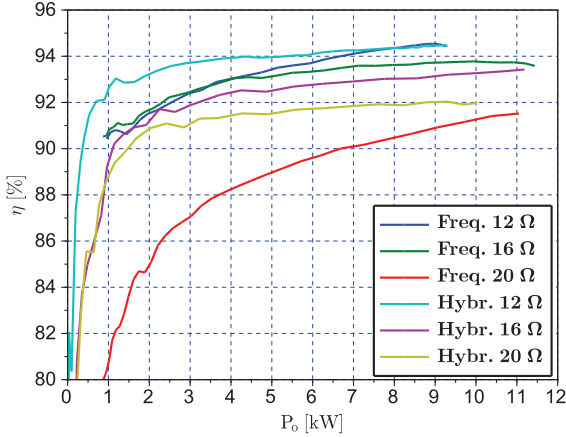


Fig. 5. System efficiency (dc-dc) for the experimental prototype with two control strategies (frequency control and phase-frequency hybrid control) and various load resistances.

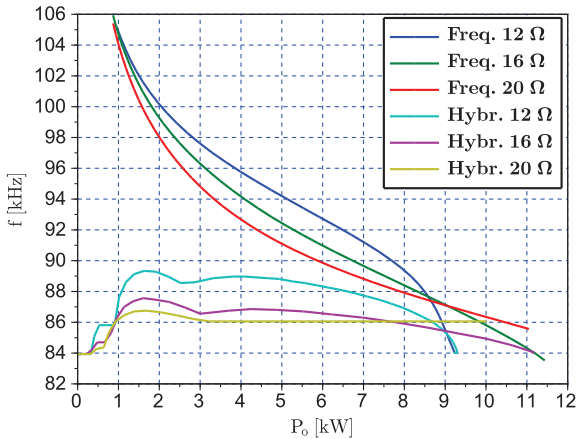


Fig. 6. Inverter operating frequency for the experimental prototype with two control strategies (frequency control and phase-frequency hybrid control) and various load resistances.

The next three plots show results of a comparison between frequency control and hybrid control strategies. The dc-dc system efficiency for these two types of control is shown in Fig. 5. It can be observed that for most cases the efficiency is higher for hybrid control strategy. Fig. 6 shows the inverter operating frequencies for the two compared cases. It clearly illustrates that the hybrid control allows for keeping the operating frequency within limited range in the whole regulation range. The hybrid control also does not have low-power operation limitations. As opposed to the frequency control which requires very high frequencies at low power, the proposed hybrid control strategy regulates from no power to full load in a narrow frequency range. The graph shown in Fig. 7 presents phase currents of the inverter for hybrid control and 12 Ω load resistance. It can be seen that currents differ from one another.

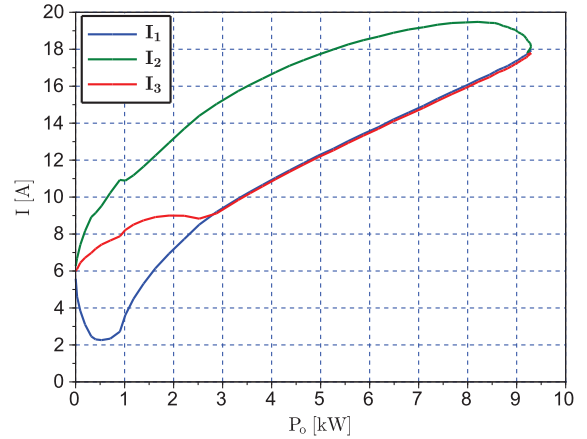


Fig. 7. Inverter phase current rms values for the experimental prototype for phase-frequency hybrid control) and 12 Ω load resistance.

Phase 2 current is always significantly higher than the other two currents. It is related to the circulating currents between the inverter phases.

## V. CONCLUSIONS

In this paper, a three-phase resonant inverter for wireless power transfer applications is presented. A new approach to control strategies has been proposed and implemented. A laboratory prototype was built and tested to verify the proposed concepts. Experimental results showed that the proposed hybrid phase-frequency control strategy performs well. The experiment also proved the advantages of the proposed concept over traditional frequency controlled inverters. Firstly, the proposed concept provides full-range regulation from zero to full power without losing ZVS conditions. Secondly, it keeps the operating frequency range narrow, in particular, it can operate within the frequency range suggested by SAE J2954 for wireless charging electric vehicles. And thirdly, the presented inverter has high efficiency in a wide range of operation parameters.

## VI. ACKNOWLEDGMENT

This work was supported by PowerBridgeNY program.

## REFERENCES

- [1] O. Lazaro and G. A. Rincon-Mora, "A nonresonant self-synchronizing inductively coupled 0.18- $\mu\text{m}$  CMOS power receiver and charger," *IEEE Journal of Emerging and Selected Topics in Power Electronics*, vol. 3, no. 1, pp. 261-271, Mar. 2015.
- [2] J. M. Miller, O. C. Onar, and M. Chinthavali, "Primary-side power flow control of wireless power transfer for electric vehicle charging," *IEEE Journal of Emerging and Selected Topics in Power Electronics*, vol. 3, no. 1, pp. 147-162, Mar. 2015.
- [3] M. Zargham and P. G. Gulak, "Fully integrated on-chip coil in 0.13 $\mu\text{m}$  CMOS for wireless power transfer through biological media," *IEEE Transactions on Biomedical Circuits and Systems*, in press.
- [4] O. Knecht, R. Bosshard, and J. Kolar, "High efficiency transcutaneous energy transfer for implantable mechanical heart support systems," *IEEE Transactions on Power Electronics*, in press.
- [5] J. Kuipers, H. Bruning, D. Yntema, S. Bakker, and H. Rijnaarts, "Self-capacitance and resistive losses of saline-water-filled inductors," *IEEE Transactions on Industrial Electronics*, vol. 61, no. 5, pp. 2356-2361, May 2014.

- [6] D. Kurschner, C. Rathge, and U. Jumar, "Design methodology for high efficient inductive power transfer systems with high coil positioning flexibility," *IEEE Transactions on Industrial Electronics*, vol. 60, no. 1, pp. 372-381, Jan. 2013.
- [7] R. M. Bergonsi, D. W. Ferreira, and L. Lebensztajn, "Modeling coreless transformers with a relatively large wire gauge using an optimization method," *IEEE Transactions on Magnetics*, vol. 50, no. 2, pp. 981-984, Feb. 2014.
- [8] A. Collado and A. Georgiadis, "Optimal waveforms for efficient wireless power transmission," *IEEE Microwave and Wireless Components Letters*, vol. 24, no. 5, pp. 354-356, May 2014.
- [9] J. F. Sanz, J. L. Villa, J. Sallan, J. M. Perie, and L. G. Duarte, "UNPLUGGED Project: development of a 50 kW inductive electric vehicle battery charge system," *EV27 Electric Vehicle Symposium and Exhibition*, Nov. 2013.
- [10] R. Bosshard, J. W. Kolar, and B. Wunsch, "Accurate finite-element modeling and experimental verification of inductive power transfer coil design," *IEEE Applied Power Electronics Conference and Exposition*, pp. 1648-1653, Mar. 2014.
- [11] H. H. Wu, A. Gilchrist, K. D. Sealy, and D. Bronson, "A high efficiency 5 kW inductive charger for EVs using dual side control," *IEEE Transactions on Industrial Informatics*, vol. 8, no. 3, pp. 585-595, Aug. 2012.
- [12] I. Fujita, T. Yamanaka, Y. Kaneko, S. Abe, and T. Yasuda, "A 10 kW transformer with a novel cooling structure of a contactless power transfer system for electric vehicles," *IEEE Energy Conversion Congress and Exposition*, pp. 3643-3650, Sep. 2013.
- [13] J. Huh, S. W. Lee, W. Y. Lee, G. H. Cho, C. T. Rim, "Narrow-width inductive power transfer system for online electrical vehicles," *IEEE Transactions on Power Electronics*, vol. 26, no. 12, pp. 3666-3679, Dec. 2011.
- [14] J. Shin, S. Shin, Y. Kim, S. Ahn, S. Lee, G. Jung, S. J. Jeon, and D. H. Cho, "Design and implementation of shaped magnetic resonance based wireless power transfer system for roadway powered moving electric vehicles," *IEEE Transactions on Industrial Electronics*, vol. 61, no. 3, pp. 1179-1192, Mar. 2014.
- [15] M. Jurjevich, "Large-scale, commercial wireless inductive power transfer (WPT) for fixed route bus rapid transportation", *IEEE Transportation and Electrification Newsletter*, Oct. 2014.
- [16] M. Bojarski, E. Asa, and D. Czarkowski, "Effect of wireless power link load resistance on the efficiency of the energy transfer," in *Proc. IEEE International Electric Vehicle Conference (IEVC)*, Dec. 2014.
- [17] M. Bojarski, D. Czarkowski, F. de Leon, Q. Deng, M. K. Kazimierczuk, and H. Sekiya, "Multiphase resonant inverters with common resonant circuit," in *Proc. IEEE International Symposium on Circuits and Systems (ISCAS)*, pp. 2445-2448, Jun. 2014.
- [18] M. Bojarski, K. K. Kutty, D. Czarkowski, and F. de Leon, "Multiphase resonant inverters for bidirectional wireless power transfer," in *Proc. IEEE International Electric Vehicle Conference (IEVC)*, Dec. 2014.